Differential Aberration in WISE Images

Document number: WSDC-D-T034

1. Overview

The motion of the WISE telescope relative to the J2000 coordinate system induces a shift in the apparent position of celestial objects expressed in that system. This is caused by the *aberration* of light rays entering the telescope. This effect follows from the fact that light travels with finite speed, and therefore during the time it takes a photon to travel a given distance, the telescope itself moves by an amount proportional to its speed in the reference frame. This results in a slight shift in apparent direction that depends on the angle between the line of sight and the velocity vector. Since WISE positions are calibrated against astrometric standard stars, and since the positions of those stars as observed by WISE are similarly affected by aberration, all celestial objects in the field of view are shifted by approximately the same amount, and J2000 position error due to aberration is almost canceled. This is only approximate, however, because a given pixel's line of sight depends on the pixel's location in the array, and so the exact relationship between line of sight and the velocity vector varies over the array. The resulting pixel-to-pixel variation of aberration is called *differential aberration*.

Because each pixel experiences aberration that is generally different from that of other pixels, in effect a very small distortion is induced in the mapping between pixel array coordinates and celestial position. For WISE, this distortion has a maximum amplitude of several tenths of an arcsecond. This is below the mission requirement on position reconstruction accuracy, but not orders of magnitude below it, and for typical source densities, the PRex processing is capable of detecting it. Since it is a purely geometrical effect, it can be computed theoretically and removed by including its effects on the total distortion model. This is preferable to removing it as a time-dependent scale-factor variation calibrated by PRex, since the latter depends on WISE source detections whose extracted positions have an error dispersion that adds noise to the calibration, whereas the theoretical model is limited only by negligible approximation errors (e.g., the use of the nonrelativistic formula for aberration, which is entirely satisfactory for the velocities involved in this case). Furthermore, this is the only known source of distortion that varies with time on as short a scale as the orbital period, and by including it in the total distortion model at the top of the processing chain, time-dependent distortion effects are made transparent to the downstream modules.

2. Geometrical Derivation

Although it was discovered and satisfactorily explained (within the context of Newtonian physics) by James Bradley in 1725, light aberration is actually a relativistic effect, and in 1905 Einstein used

special relativity to derive the formula

$$\cos\theta_o = \frac{\cos\theta_s - \frac{v}{c}}{1 - \frac{v}{c}\cos\theta_s} \qquad (1)$$

where θ_o and θ_s are angles measured in the plane containing the line of sight and the velocity vector with magnitude v, c is the speed of light, the subscript o denotes the angle between the velocity vector and the direction where the observed object would appear to be if the speed of light were infinite, and the subscript s denotes the corresponding angle where the object actually appears to be, given that the speed of light is finite.

For WISE, the relevant velocity is the sum of the spacecraft velocity in its orbit about Earth and the velocity of Earth in its orbit about the sun. This results from the fact that WISE positions are expressed in J2000, which is an inertial sun-centered coordinate system. In other words, the relevant velocity is that relative to the coordinate system in use. If, for example, the coordinate system were an inertial system at rest with respect to the Milky Way, then the velocity of the sun about the Galactic center would enter and result in vastly larger aberration, most of which is the same for the sun and the spacecraft.

So the value of v varies between about 22.3 to 37.4 km/s, for which v/c is on the order of 10^{-4}. We can safely ignore relativistic effects, therefore, and the following approximation based on simple trigonometry is completely satisfactory. This is just the formula one would derive using classical physics for the problem usually employed for visualizing aberration, that of a person with an umbrella in rain that is falling at some known angle in the rest frame of a street. It is easiest to visualize for the case in which the rain is falling vertically. If the person is standing still, the umbrella is best pointed straight up. If the person is walking with speed v_p, and the rain is falling with speed v_r, then the umbrella is best pointed forward at an angle θ from the vertical, where $\tan\theta = v_p/v_r$.

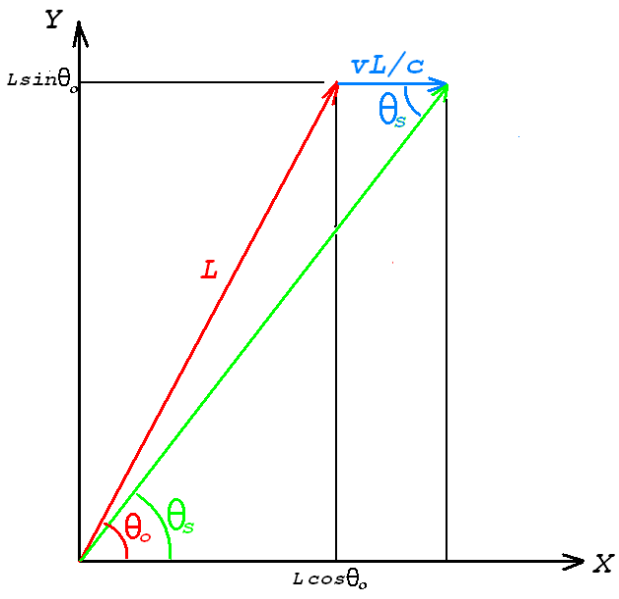

For the more general case in which the rain is falling at some angle other than the vertical, some trigonometry is needed to derive the relationship between the angle of the rain in the rest frame and that in the moving frame. We will also switch from an umbrella to a telescope and from rain to light arriving from the direction of an observed object. The diagram on the left shows a vector of arbitrary length L at an angle θ_o pointing in the direction of the observed object as measured in the rest frame, the XY coordinates. The telescope moves in the X direction with speed v. It takes light a time L/c to travel the distance L (which is going to cancel out below), and during this time, the telescope moves a distance vL/c, making the object appear to be at the angle θ_s. The tangent of θ_s is seen to be:

$$\tan\theta_s = \frac{L\sin\theta_o}{L\cos\theta_o + \dfrac{vL}{c}} = \frac{\sin\theta_o}{\cos\theta_o + \dfrac{v}{c}} \tag{2}$$

This equation is completely adequate for the nonrelativistic case. We may inspect the shift itself more closely by defining $\Delta\theta \equiv \theta_o - \theta_s$ and then using the law of sines:

$$\frac{\dfrac{vL}{c}}{\sin\Delta\theta} = \frac{L}{\sin\theta_s} \tag{3}$$

Then canceling L and re-arranging yields

$$\sin\Delta\theta = \frac{v}{c}\sin\theta_s \tag{4}$$

In nonrelativistic applications, $\Delta\theta$ is usually small enough to use $\Delta\theta \approx \sin\Delta\theta$, and furthermore, the distinction between $\sin\theta_s$ and $\sin\theta_o$ in Equation 4 can usually be ignored at the cost of a maximum relative error of order about v/c. That may be useful when only the rest-frame angle θ_o is known; if greater accuracy is needed, then either iterating Equation 4 or simply using Equation 2 is advisable.

3. WISE Processing

During the in-orbit-checkout calibration of distortion (see J. Fowler *et al.*, *WSDC-D-T033*), variations in the plate scales were observed with a one-orbit period. The period was deduced from plots of scale-factor corrections versus time and versus ecliptic latitude of the telescope boresight. The latter are more revealing, since they combine data from many orbits. The plot below shows the variation in X scale factor correction as a function of ecliptic latitude. These data cover the 14 orbits of Julian Day number 2455282. Results from ascending scans are shown in blue, descending in red. Each point is an average over 4 degrees containing approximately 78 frames. Except for some residual noise and a few outliers, the data behave exactly as differential aberration predicts, with negligible change from the mean scale factor at the poles and a relative correction of magnitude

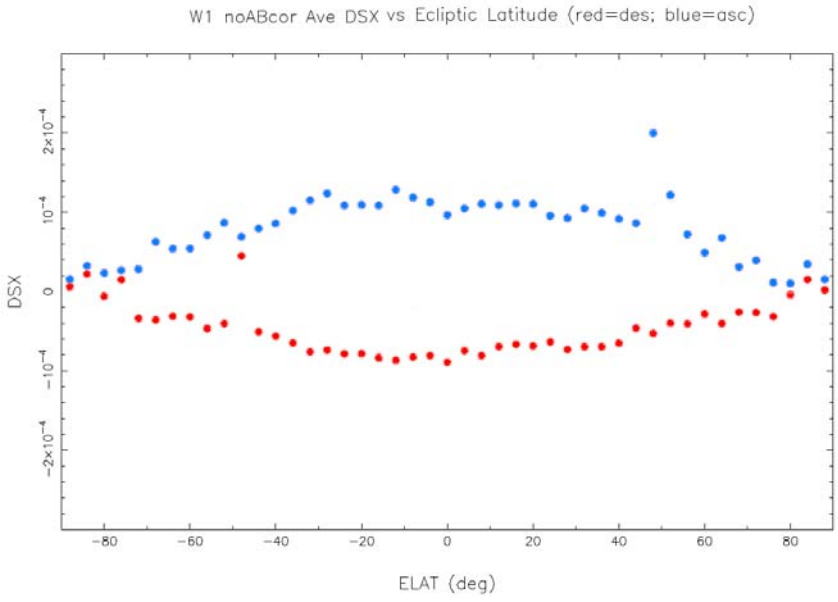

about 10^{-4} in the ecliptic.

To compute aberration, the velocity vector of the spacecraft in J2000 is needed. This is supplied in the FITS headers of each frame via the parameters SCVELX, SCVELY, and SCVELZ, in units of AU/day. This vector will be denoted (V_x, V_y, V_z). This must be mapped into frame coordinates, whose RA, Dec, and Twist are obtained from the FITS header parameters CRVAL1, CRVAL1, and WCROTA2, denoted (α, δ, γ). A transformation matrix is defined as follows: starting with a Cartesian *XYZ* system whose *Z* axis points to the celestial north pole and whose *X* axis points to the vernal equinox, we perform three Euler rotations as follows, where we will use α = 120°, δ = 60°, and γ = 30° for illustration.

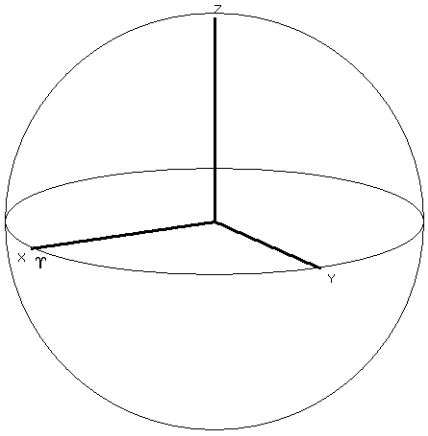

$\varphi_1 = \alpha - 90^\circ$ about *Z* :

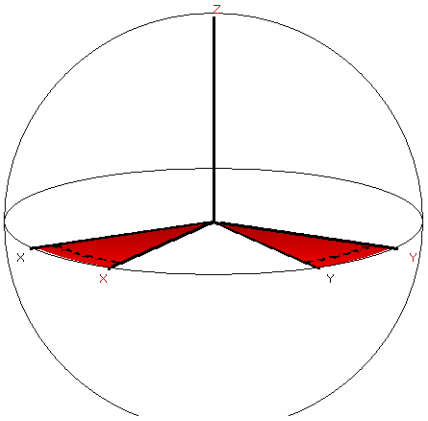

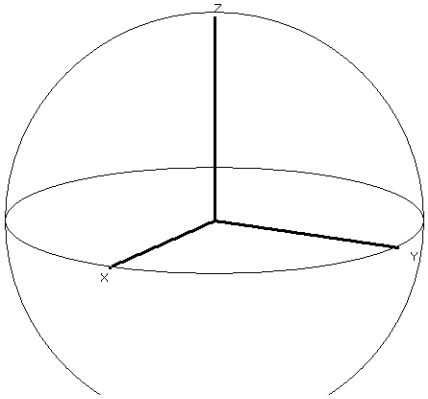

$\varphi_2 = \delta - 90^\circ$ about *X* :

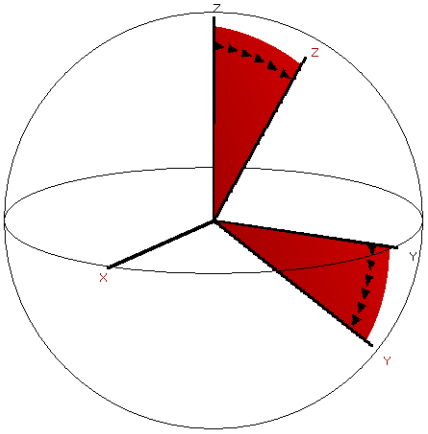

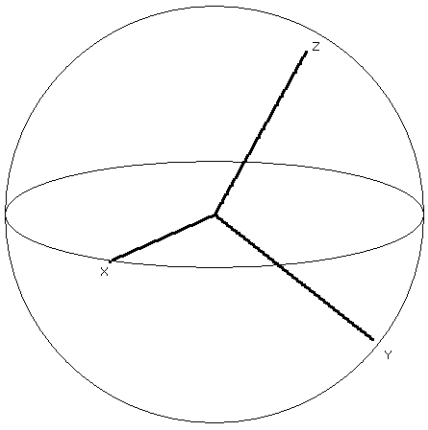

$\varphi_3 = \gamma + 180^\circ$ about *Z*:

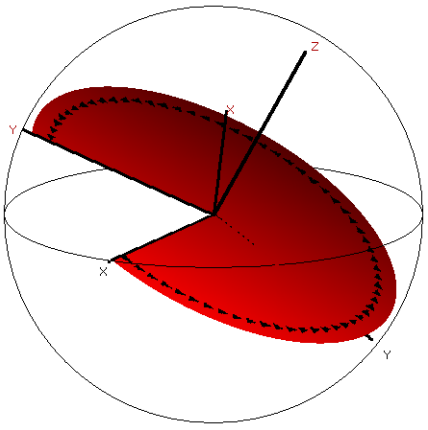

This places the *Z* axis on the celestial position (α, δ) with the *Y* axis aligned with the array's *Y* axis. The three rotations yield the following transformation matrix.

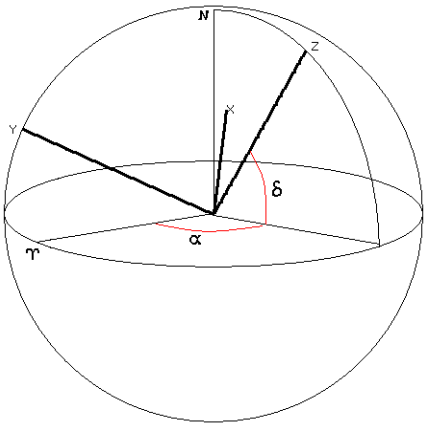

$$T \equiv \begin{pmatrix} T_{11} & T_{12} & T_{13} \\ T_{21} & T_{22} & T_{23} \\ T_{31} & T_{32} & T_{33} \end{pmatrix}$$

$$= \begin{pmatrix} \cos\varphi_3 & \sin\varphi_3 & 0 \\ -\sin\varphi_3 & \cos\varphi_3 & 0 \\ 0 & 0 & 1 \end{pmatrix} \begin{pmatrix} 1 & 0 & 0 \\ 0 & \cos\varphi_2 & \sin\varphi_2 \\ 0 & -\sin\varphi_2 & \cos\varphi_2 \end{pmatrix} \begin{pmatrix} \cos\varphi_1 & \sin\varphi_1 & 0 \\ -\sin\varphi_1 & \cos\varphi_1 & 0 \\ 0 & 0 & 1 \end{pmatrix}$$

$$\begin{aligned}
T_{11} &= \cos\varphi_3 \cos\varphi_1 - \sin\varphi_3 \cos\varphi_2 \sin\varphi_1 \\
T_{12} &= \cos\varphi_3 \sin\varphi_1 + \sin\varphi_3 \cos\varphi_2 \cos\varphi_1 \\
T_{13} &= \sin\varphi_3 \sin\varphi_2 \\
T_{21} &= -\sin\varphi_3 \cos\varphi_1 - \cos\varphi_3 \cos\varphi_2 \sin\varphi_1 \\
T_{22} &= -\sin\varphi_3 \sin\varphi_1 + \cos\varphi_3 \cos\varphi_2 \cos\varphi_1 \\
T_{23} &= \cos\varphi_3 \sin\varphi_2 \\
T_{31} &= \sin\varphi_2 \sin\varphi_1 \\
T_{32} &= -\sin\varphi_2 \cos\varphi_1 \\
T_{33} &= \cos\varphi_2
\end{aligned} \tag{5}$$

This corresponds to a *Z* axis that looks outward from the origin, whereas the band-frame coordinates look in from the sky. The *X* and *Z* axes must be reflected; this will be taken into account via the fact that the angular scale factor on *X* is negative. The *Z* reflection can be ignored, because that axis is the line of sight, and only the sine of the angle between a line of sight and the velocity vector comes into play, and $\sin\theta = \sin(180^\circ - \theta)$. Technically, we are not using band-frame coordinates as defined in the PRex subsystem, so we will refer to this system simply as the "frame system" (e.g., band-frame pixel coordinates run from 1 to 1016 in W1-W3, whereas our origin is the Z axis, and so pixel coordinates run from -507.5 to +507.5; appropriate adjustments are made for W4). The frame-system components of the velocity vector are therefore

$$\begin{pmatrix} V_{fx} \\ V_{fy} \\ V_{fz} \end{pmatrix} = \begin{pmatrix} T_{11} & T_{12} & T_{13} \\ T_{21} & T_{22} & T_{23} \\ T_{31} & T_{32} & T_{33} \end{pmatrix} \begin{pmatrix} V_x \\ V_y \\ V_z \end{pmatrix} \tag{6}$$

The Z axis of the frame-system coordinates is the line of sight from the center of the array, so the velocity vector (V_{fx}, V_{fy}, V_{fz}) defines the magnitude and direction of the velocity with respect to the array center. For a given frame, the time tag is taken to be the midpoint of the photometric integration period, and so the velocity vector is essentially the average over that period, but changes in magnitude and direction are small enough to ignore. The magnitude changes typically by about 60 m/s frame-to-frame, or 0.2%. The angle relative to Z typically changes by a few tenths of a degree. Using the average over such small changes should have an approximation error at least an order of magnitude smaller, so that differential aberration effects of 0.25 arcsec should be computed with an accuracy better than 0.5 milli-arcsec.

The velocity magnitude extrema occur when the telescope is observing the ecliptic poles. The orbital geometry results in a maximum total velocity of 37.4 km/s in the north, where the spacecraft's velocity about the Earth adds to the Earth's velocity about the sun. At the south pole, the former subtracts from the latter, producing a magnitude of 23.4 km/s. The maximum total aberration is therefore at the ecliptic north pole, with a magnitude of 25.74 arcsec. As Equation 4 shows, the aberration peaks where $\sin\theta_s$ peaks, and at the north pole, $\theta_s = 90^o$, and v/c also peaks there. But we saw that the scale-factor variations are *minimal* at the poles; that is because they depend on *differential* aberration, not total aberration. Since the aberration varies as $\sin\theta_s$, its differential varies as $\cos\theta_s$, which is maximal in *magnitude* near the ecliptic plane (it is not quite *in* the ecliptic because of the spacecraft velocity about the Earth). Note that we will not use the $\cos\theta_s$ dependence explicitly; if we did, we *would* have to reflect Z, but we will compute differential aberration numerically as the difference between total aberration at two points in the array (see Equation 7 below).

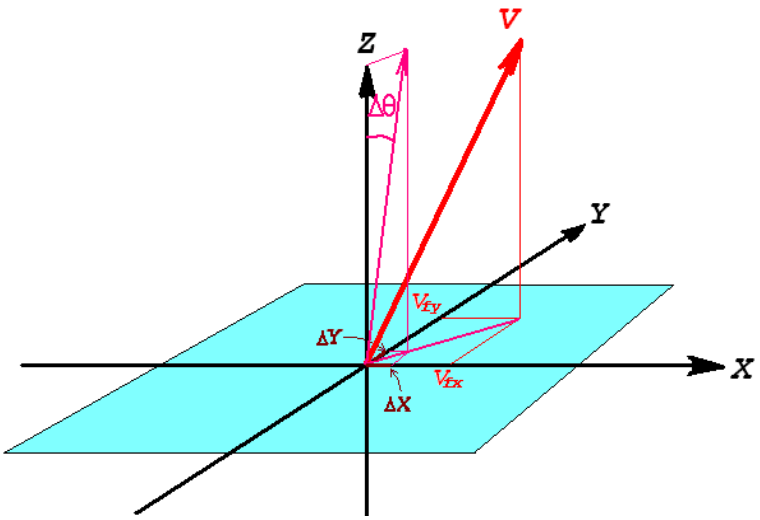

The figure on the left illustrates a velocity vector V mapped into frame-system coordinates. The line of sight of the center of the array is the Z axis in the rest frame of the array. The presence of the velocity vector shifts that line of sight in the J2000 system by the amount $\Delta\theta$ in the plane containing Z and V. This angular shift translates into pixel shifts on the X and Y axes, indicated in the figure by ΔX and ΔY, respectively. These components are in the same proportion as V_{fx} and V_{fy} (the components of V on the X and Y axes).

We compute differential aberration for a given pixel by computing the total aberration for that pixel and subtracting the total aberration for the center of the array, i.e., the frame-system Z axis. This results in differential aberration being defined to be zero at the center of the array. The total aberration there is computed by using Equation 4 with θ_s approximated as the angle between V and Z (i.e., θ_o) and with the small-angle approximation $\Delta\theta \approx \sin\Delta\theta$:

$$
\begin{aligned}
U &\equiv \frac{1}{|V|}\begin{pmatrix} V_{fx} \\ V_{fy} \\ V_{fz} \end{pmatrix} = \begin{pmatrix} U_x \\ U_y \\ U_z \end{pmatrix} \\
\theta &= \cos^{-1}(U \bullet Z) \\
\Delta\theta &= \frac{v}{c}\sin\theta \\
w_x &\equiv \frac{U_x}{\sqrt{U_x^2 + U_y^2}} \quad , \quad w_y \equiv \frac{U_y}{\sqrt{U_x^2 + U_y^2}} \\
\Delta X &= w_x \Delta\theta \, , \Delta Y = w_y \Delta\theta
\end{aligned}
\tag{7}
$$

Sensitivity testing has shown that in double precision, the use of the dot product to obtain the angle is sufficiently accurate over the entire range of angles involved. As shown, ΔX and ΔY are in radian units; they can be rescaled to pixel units to sufficient accuracy by using the nominal pixel scale.

The total aberration of a given pixel with frame-system coordinates (X,Y) is computed in exactly the same way after first rotating the coordinate system to one in which that pixel's line of sight is the Z axis. This is one of several methods that account for the fact that when V is nearly parallel (or antiparallel) to the frame-system Z axis (i.e., when differential aberration is maximal for a given velocity magnitude), the aberration direction components w_x and w_y for a given pixel are highly sensitive to the pixel's position the array.

This rotation employs small angles, and therefore we can ignore the order in which the rotations are done. We will use $(\varphi_x,\varphi_y) = (S_x \times X, S_y \times Y)$ in radian units, where S_x and S_y are the angular scales on the X and Y axes, respectively (recall that S_x is negative). Technically this would require employing the full distortion model, since optical distortion can cause pixel line-of-sight shifts up to the equivalent of several pixels in the corners. The *difference* in aberration between points two pixels apart (i.e., 5-7 arcseconds) is quite small, however, and so we expect that this can be ignored as a second-order effect in an already-small phenomenon. Furthermore, this much optical-distortion shift affects only a small minority of the points that go into the fitting.

The (X,Y) coordinates of the array location whose line of sight is the Z axis are (0,0). To rotate the Z axis to a direction corresponding to an arbitrary (X,Y) location, we can rotate about the Y axis by the angle φ_x and then rotate about the X axis by the angle $-\varphi_y$. These rotations can be done in either order, because the rotation angles are very small, and so rotations commute to sufficient accuracy (sensitivity testing revealed maximum aberration errors at the milli-arcsec level over the range of realistic cases). The two rotation matrices are:

$$R_y = \begin{pmatrix} \cos\varphi_x & 0 & -\sin\varphi_x \\ 0 & 1 & 0 \\ \sin\varphi_x & 0 & \cos\varphi_x \end{pmatrix}$$

$$R_x = \begin{pmatrix} 1 & 0 & 0 \\ 0 & \cos\varphi_y & -\sin\varphi_y \\ 0 & \sin\varphi_y & \cos\varphi_y \end{pmatrix} \tag{8}$$

Applying these to the T matrix in the order shown gives the transformation T' from celestial Cartesian coordinates to a frame system whose Z axis is the selected pixel's line of sight:

$$\begin{aligned}
T' &= R_x\, R_y\, T \\
T'_{11} &= T_{11}\cos\varphi_x - T_{31}\sin\varphi_x \\
T'_{12} &= T_{12}\cos\varphi_x - T_{32}\sin\varphi_x \\
T'_{13} &= T_{13}\cos\varphi_x - T_{33}\sin\varphi_x \\
T'_{21} &= -T_{11}\sin\varphi_y\sin\varphi_x + T_{21}\cos\varphi_y - T_{31}\sin\varphi_y\cos\varphi_x \\
T'_{22} &= -T_{12}\sin\varphi_y\sin\varphi_x + T_{22}\cos\varphi_y - T_{32}\sin\varphi_y\cos\varphi_x \\
T'_{23} &= -T_{13}\sin\varphi_y\sin\varphi_x + T_{23}\cos\varphi_y - T_{33}\sin\varphi_y\cos\varphi_x \\
T'_{31} &= T_{11}\cos\varphi_y\sin\varphi_x + T_{21}\sin\varphi_y + T_{31}\cos\varphi_y\cos\varphi_x \\
T'_{32} &= T_{12}\cos\varphi_y\sin\varphi_x + T_{22}\sin\varphi_y + T_{32}\cos\varphi_y\cos\varphi_x \\
T'_{33} &= T_{13}\cos\varphi_y\sin\varphi_x + T_{23}\sin\varphi_y + T_{33}\cos\varphi_y\cos\varphi_x
\end{aligned} \tag{9}$$

The T' matrix is then used instead of the T matrix in Equation 6 to get the velocity components in this pixel-centered system. These components are then used as shown in Equation 7 to get the total aberration components for the given pixel, which we will denote ΔX_p and ΔY_p, respectively. The differential aberration, denoted δX_p and δY_p, is then

$$\begin{aligned}
\delta X_p &= \Delta X_p - \Delta X \\
\delta Y_p &= \Delta Y_p - \Delta Y
\end{aligned} \tag{10}$$

4. Correcting for Differential Aberration

It was decided to correct for differential aberration early in the WSDC pipeline so that all downstream processing would be based on focal-plane geometry not distorted by this effect. The distortion can be approximated well by a first-order polynomial in X and Y, since the entire significant extent of the phenomenon manifests as a change in plate scale. The program `diffabr8` was designed to accomplish the correction by preprocessing the L1A frames as follows:

A.) Read the FITS header to obtain: the J2000 instrument angles CRVAL1, CRVAL2, and WCROTA2; the J2000 spacecraft velocity vector SCVELX, SCVELY, and SCVELZ; the band number BAND (needed for mapping W4 correctly in step D below).

B.) Construct the instrument Cartesian coordinate system (Equation 5) and map the spacecraft velocity vector into it (Equation 6).

C.) Compute the central aberration (Equation 7).

D.) Loop over a two-dimensional 31×31 grid of equally spaced (X, Y) locations that uniformly span the array; for each location, compute the differential aberration $(\delta X_p, \delta Y_p)$ (Equations 8-10) and store in arrays *ImgX* and *ImgY*, respectively.

E.) Use the *ImgX* and *ImgY* arrays in separate first-order polynomial fits to obtain the coefficients *dA00*, *dA01*, *dA10*, *dB00*, *dB01*, and *dB10* (see Appendix A):

$$\begin{aligned} du &= -\delta X_p = dA00 + dA01\,Y + dA10\,X \\ dv &= -\delta Y_p = dB00 + dB01\,Y + dB10\,X \end{aligned} \tag{11}$$

where the minus signs enter in order to be consistent with the definition used for distortion.

F.) An ingest utility then reads the stdout from `diffabr8` and reads the FITS header to obtain the SIP coefficients below second order, A_0_0, A_0_1, A_1_0, B_0_0, B_0_1, B_1_0, AP_0_0, AP_0_1, AP_1_0, BP_0_0, BP_0_1, and BP_1_0; it then modifies these coefficients as follows:

A_0_0 ← A_0_0 + dA00
A_0_1 ← A_0_1 + dA01
A_1_0 ← A_1_0 + dA10
B_0_0 ← B_0_0 + dB00
B_0_1 ← B_0_1 + dB01
B_1_0 ← B_1_0 + dB10
AP_0_0 ← AP_0_0 - dA00
AP_0_1 ← AP_0_1 - dA01
AP_1_0 ← AP_1_0 - dA10
BP_0_0 ← BP_0_0 - dB00
BP_0_1 ← BP_0_1 - dB01
BP_1_0 ← BP_1_0 - dB10

5. Examples

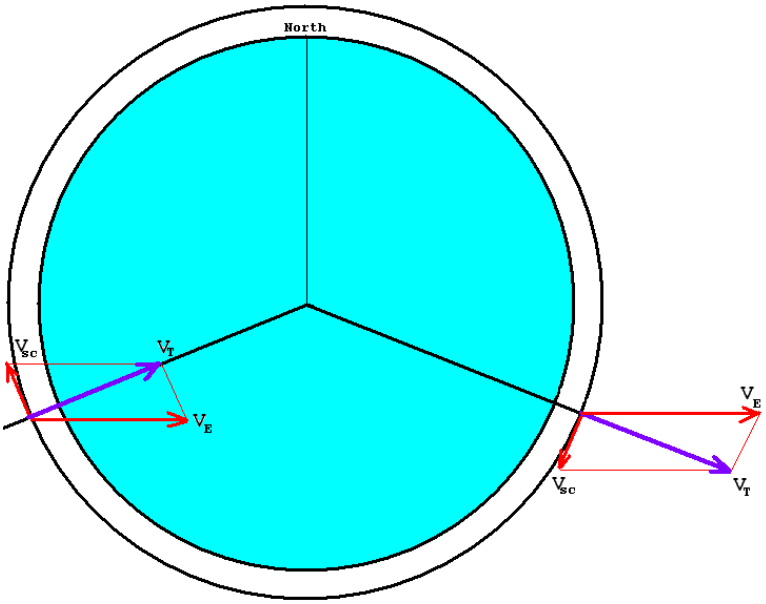

Differential aberration is minimal near the ecliptic poles and maximal in the ecliptic, despite the fact that $\cos\theta_s$ is *not* maximal there; $\cos\theta_s$ is maximal at $\theta_s = 0$, where the sum of the Earth's velocity around the sun and the spacecraft's velocity about the Earth combine to make the total velocity as nearly parallel as possible to the telescope boresight. The schematic on the left illustrates this; V_{sc} is the spacecraft velocity about the Earth, V_E is the Earth's velocity around the sun, and V_T is the total velocity. The latitude at which $\theta_s = 0$ is about -15°, but at that point the total velocity has dropped from about 30.6 km/s with the line of sight in the ecliptic to about 28.6 km/s at this latitude (using average velocities), because the spacecraft's geocentric velocity subtracts from the Earth's heliocentric velocity. The loss of total velocity by a factor of 0.9355 overcomes the gain in $\cos\theta_s$ from about 0.9685 in the ecliptic to 1.0 at this latitude, so the differential aberration is not maximal there; the ecliptic wins because of the higher total velocity. The diagram should not be taken to suggest that the spacecraft passes over the Earth's north pole, of course, since the orbital inclination places the orbit plane about 7 degrees off the pole.

Furthermore there are seasonal variations in the relationship between the telescope line of sight and the local normal. The diagram below shows the orbital plane and Earth's terminator at the northern-hemisphere winter and summer solstices. The orbital plane is tied to the Earth's geographical frame, maintaining the 7 degree inclination throughout the year but precessing at essentially the same rate as the Earth's angular revolution around the sun.

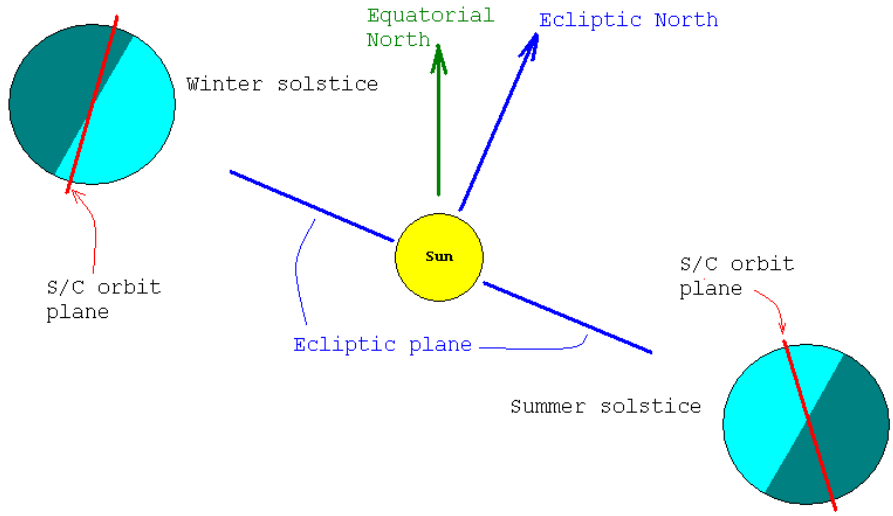

When passing through its closest approach to the Earth's north pole, the telescope look direction is parallel to the Ecliptic North vector; clearly it is looking out of the orbit plane much more near summer solstice than near winter solstice. So the relationship between telescope look direction and total velocity vector undergoes significant seasonal variations, and these produce seasonal variations in the differential aberration, although not with much amplitude. In addition, the spacecraft spends some time in Earth's shadow near summer solstice.

The size of the differential aberration effects are practically symmetric about the ecliptic plane. For $\pm\Delta$ ecliptic latitude, above the plane, the total velocity is larger while $\cos\theta_s$ is smaller; at the same distance below the plane, $\cos\theta_s$ has grown larger by the same amount as the total velocity has grown smaller, yielding the same amount of differential aberration. This symmetry, and also the amount of seasonal variation, can be seen in this plot of theoretical relative array Y-axis scale-factor change as a function of ecliptic latitude for real WISE frame data uniformly sampled between just after winter solstice through summer solstice (January 14, 2010, survey start, through June 21, 2010).

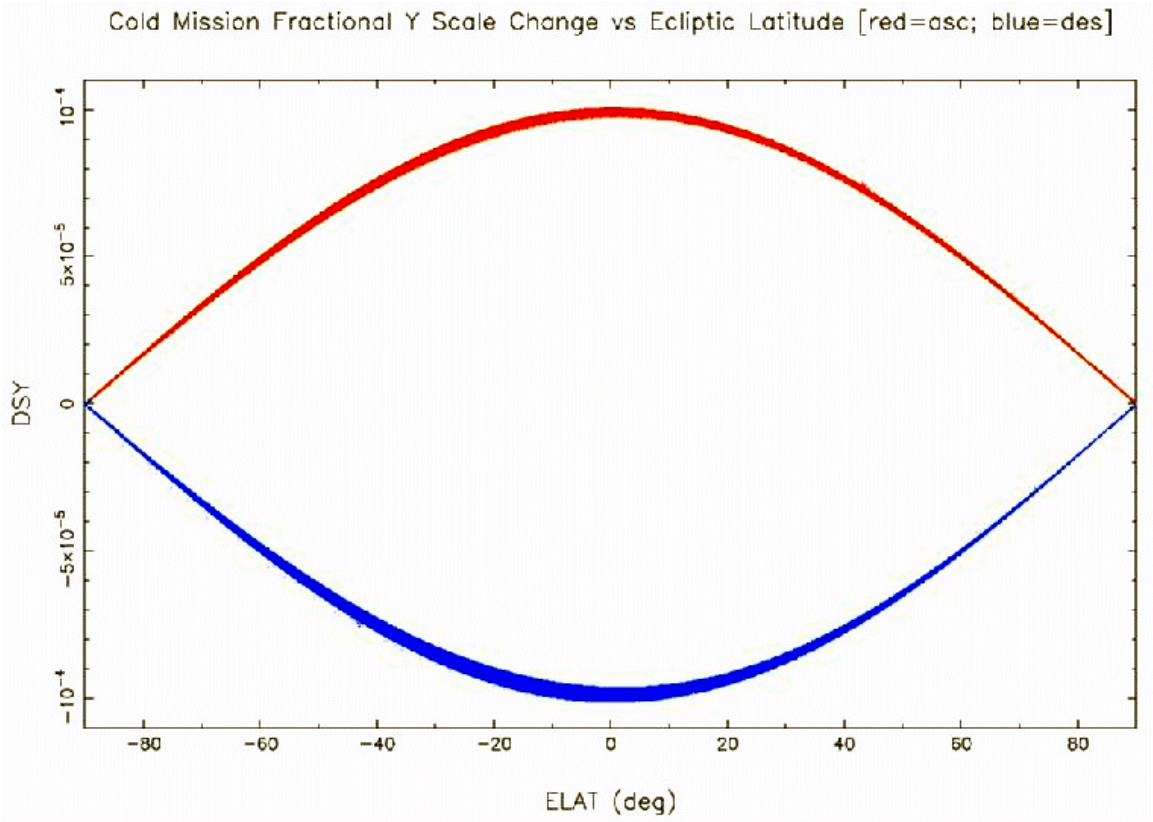

This can be compared to the plot in section 3 (note the switch in color assignments, however). The variation in thickness is due to the seasonal variations. The inside edges come from summer solstice, and the outer edges come from winter solstice. Since the telescope scans very close to the terminator meridian, when it passes through the ecliptic, it is always looking almost parallel or antiparallel to the Earth's velocity vector around the sun, but at summer solstice the Earth is only about two weeks from aphelion, and so that velocity has a magnitude of only 97.4% of the winter-solstice magnitude, slightly lowering the aberration effects. It is also seen that the effects for ascending scans are

opposite those for descending scans. This is because the effect of aberration is to shift the apparent position toward the velocity vector. On descending scans, this is not far from the array-center line of sight, so that edge pixels shift their view toward the center, reducing the effective plate scale. On ascending scans, the velocity vector points more nearly toward the opposite side of the sky from the look direction, and so edge pixels shift their view away from the center of the array, increasing the effective plate scale.

The shape of the distortion induced by differential aberration can be seen in a vector-flow diagram such as used in general discussions of distortion (see "WISE IOC Distortion Calibration", Document number WSDC D-T033). A refined distortion model (relative to the IOC model) was generated from five 5-day periods uniformly sampled from the cold mission. To probe the effects of differential aberration, two full distortion fits (no precompensation for differential aberration) were generated using only frames within 20 degrees of the ecliptic; one fit used only ascending scans, and the other used only descending scans. Then the descending-scan model was subtracted from the ascending-scan model. The difference between the two models is twice the distortion induced near the ecliptic by differential aberration alone. The vector-flow diagram for the difference is shown below. The black dots are uniformly spaced pixel locations, and the red lines are the displacement vectors, which have been scaled by a factor of 250 relative to the true plate scale.

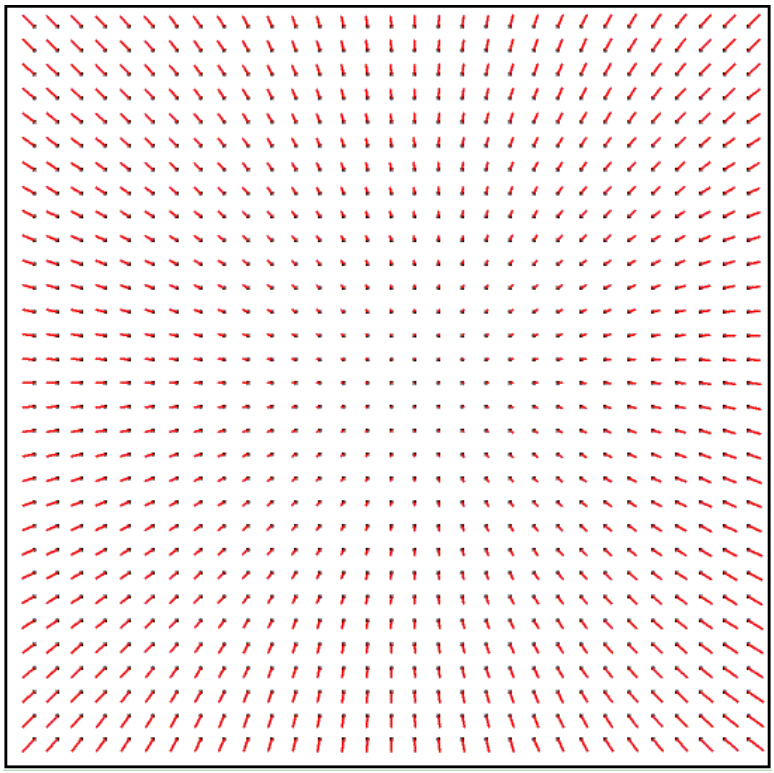

For the final products, the distortion model has been computed from WISE/2MRef sources corrected for differential aberration, i.e., the distortion model reflects what would happen if there were no differential aberration effect. Then each individual frame has the adjustment for differential aberration peculiar to its geometry made at the beginning of the processing chain. In other words,

every frame has a slightly different distortion model that corrects for both optical distortion and differential aberration. All downstream processing that uses the distortion model therefore includes correction for both effects.

The theoretical model for differential aberration is noiseless (to within some negligible approximation error) and therefore preferable to models obtained by fitting real (noisy) data, but the latter effect can be seen in the PRex calibrations for plate scale, as shown above in section 3. These effects are the same in all bands but most visible in W1 and W2 because of the greater source volume. The effects are similar on both axes, although greater residual noise is seen in W1 Y than W1 X, and in W2 X relative to W2 Y. Since the effects are similar, we will show only the W1 results here, computed from scans 06257a, 06257b, 06258a, and 06260a, with scale changes averaged inside of 10-degree-wide ecliptic latitude bins.

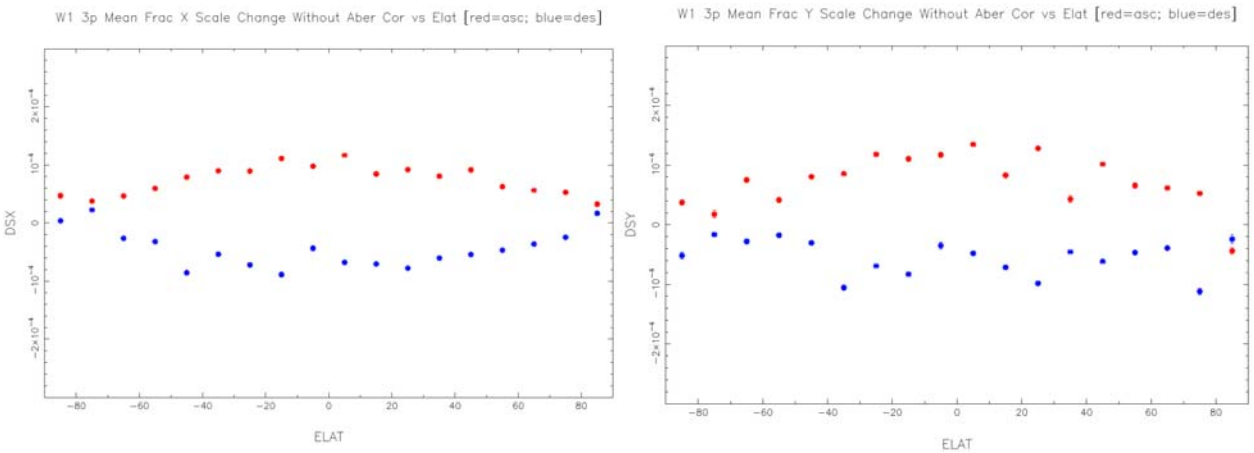

These are the scale-factor corrections that PRex (the sfprex module) would apply to correct the data, given no precompensation for differential aberration (X left, Y right).

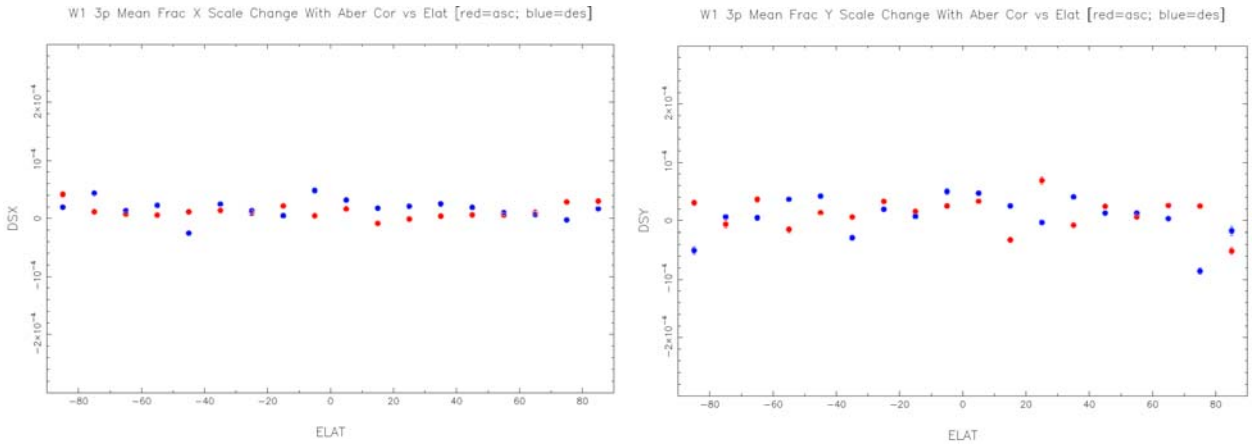

These are the scale-factor corrections that would be applied to correct the data after precompensation for differential aberration.

Appendix A: Polynomial Fit

As described in Section 4 item E (Equation 11), the differential aberration is sampled on a 31×31 grid of equally spaced (X,Y) locations that uniformly span the array, i.e., the combination of all coordinates X_i and Y_j, where i and j each run from 1 to 31. For each location, the differential aberration $(\delta X_p, \delta Y_p)_{ij}$ is computed, resulting in two grids of position offsets due to differential aberration, one for each axis. These offsets are negated and represented as du on X and dv on Y to be consistent with the gnDSTR notation. A first-order polynomial is fit to each set of offsets in the same manner for each axis, and so we will describe only the X axis herein.

To reduce clutter, we will use the notation $du = a + bY + cX$, where these coefficients are related to the SIP coefficient corrections by $a \equiv$ dA_0_0, $b \equiv$ dA_0_1, $c \equiv$ dA_1_0. The fitting dispersion to be minimized is

$$R^2 = \sum_{ij} \left(du_{ij} - (a + bY_j + cX_i) \right)^2 \tag{A.1}$$

This is equivalent to a chi-square with all the du_{ij} having the same uncertainty, which can therefore be set to unity and dropped from the notation. To minimize the dispersion, we take its derivatives with respect to the coefficients and set them to zero, obtaining

$$\begin{aligned} \sum_{ij} \left(du_{ij} - (a + bY_j + cX_i) \right) &= 0 \\ \sum_{ij} \left(du_{ij} - (a + bY_j + cX_i) \right) Y_j &= 0 \\ \sum_{ij} \left(du_{ij} - (a + bY_j + cX_i) \right) X_i &= 0 \end{aligned} \tag{A.2}$$

Regrouping,

$$\begin{aligned} aN &+ b\sum_{ij} Y_j &&+ c\sum_{ij} X_i &&= \sum_{ij} du_{ij} \\ a\sum_{ij} Y_j &+ b\sum_{ij} Y_j^2 &&+ c\sum_{ij} X_i Y_j &&= \sum_{ij} Y_j du_{ij} \\ a\sum_{ij} X_i &+ b\sum_{ij} X_i Y_j &&+ c\sum_{ij} X_i^2 &&= \sum_{ij} X_i du_{ij} \end{aligned} \tag{A.3}$$

With the definitions of a matrix $\boldsymbol{M}$ and vector $\vec{s}$,

$$M \equiv \begin{pmatrix} N & \sum_{ij} Y_j & \sum_{ij} X_i \\ \sum_{ij} Y_j & \sum_{ij} Y_j^2 & \sum_{ij} X_i Y_j \\ \sum_{ij} X_i & \sum_{ij} X_i Y_j & \sum_{ij} X_i^2 \end{pmatrix} \tag{A.4}$$

$$\vec{s} \equiv \begin{pmatrix} \sum_{ij} du_{ij} \\ \sum_{ij} Y_j du_{ij} \\ \sum_{ij} X_i du_{ij} \end{pmatrix}$$

we have

$$M \begin{pmatrix} a \\ b \\ c \end{pmatrix} = \vec{s}$$

$$\begin{pmatrix} a \\ b \\ c \end{pmatrix} = M^{-1} \vec{s} \tag{A.5}$$

$$M^{-1} = \frac{1}{D} \begin{pmatrix} M_{22} M_{33} - M_{23}^2 & M_{13} M_{23} - M_{12} M_{33} & M_{12} M_{23} - M_{13} M_{22} \\ M_{13} M_{23} - M_{12} M_{33} & M_{11} M_{33} - M_{13}^2 & M_{13} M_{12} - M_{11} M_{23} \\ M_{12} M_{23} - M_{13} M_{22} & M_{13} M_{12} - M_{11} M_{23} & M_{11} M_{22} - M_{12}^2 \end{pmatrix}$$

$$D \equiv 2 M_{13} M_{12} M_{23} - M_{22} M_{13}^2 - M_{33} M_{12}^2 - M_{11} M_{23}^2 + M_{11} M_{22} M_{33}$$

where D is the determinant of the $\boldsymbol{M}$ matrix, which is symmetric. This yields the polynomial coefficients.

References

J. Fowler, H. McCallon, **gnDSTR SDS**, WSDC D-D013.

J. Fowler, H. McCallon, **PRex SDS**, WSDC D-D003.

J. Fowler, H. McCallon, T. Conrow, F. Masci, T. Jarrett, "WISE IOC Distortion Calibration", *WSDC-D-T033*

Last update - 18 August 2011

John W. Fowler, Howard L. McCallon - IPAC